

Jon Sinnreich<sup>1\*</sup>

# The scaling effect of bored pile radius on unit shear capacity

**ABSTRACT:** The scaling effect, or influence of bored pile (drilled shaft) radius on unit shear capacity at a given displacement, is examined via a review of the literature as well as data collected in the field. It is apparent that the scaling effect of pile-soil load transfer is a measurable phenomenon on both the small scale and large scale. Since results from smaller-radius bored pile load tests are often used for the design of larger radius production piles, it may be advisable to scale down the unit shear capacity obtained from test results by the ratio of the test to production pile radii to conservatively account for the scaling effect.

**KEYWORDS:** Scaling effect, Pile unit shear

## 1. INTRODUCTION:

The scaling effect is a phenomenon in deep foundation engineering which is seemingly seldom documented in full-scale pile tests. This technical note presents some discussion of the phenomenon from the literature, and some data collected from full-scale instrumented bi-directional Osterberg Cell® (“O-cell”) test piles. Typically, larger diameter bored piles are employed in situations where larger service load settlements are expected. However, since the results of small-scale tests are often employed to validate the design of larger-scale production shafts, an awareness of the potential magnitude of the scaling phenomenon may be valuable to the design engineer. All data presented herein was collected from bored pile (drilled shaft) and auger-cast pile tests.

## 2. LITERATURE REVIEW:

The scaling effect in shear has been well documented in scale model testing (see for example Hettler (1982), Garnier and König (1998), Marandi and Karimzadeh (2009) and Vermeer and Luger (1982)).

Generally, scaling effect is attributed to one of three phenomena in the literature. The first phenomenon, of concern in scale model testing specifically, is the effect of grain size relative to the size of the model pile. Boulon and Foray (1986)

and Bałachowski (2006) used the direct shear test to simulate pile-to-soil load transfer, and concluded that the shearing occurs in a narrow band at the pile soil interface. Dilatant behavior of the sand grains within this narrow band accounts for the increase in normal stress which increases the shear stiffness. The dilatancy of the shear band in plane strain is typically modeled by use of an angle of dilatancy (e.g. Bolton (1986) and Wernick (1977), see Figure 1).

The incremental transverse dilatant shear band thickness increase  $\Delta s$  can be related to the incremental longitudinal shear displacement  $\Delta w$  via the angle of dilatancy  $\psi$ :

$$\Delta s = \Delta w \cdot \tan \psi \quad (1)$$

Because the angle of dilatancy changes with displacement, the total radial displacement  $u = \Sigma \Delta s$  up to peak dilatancy must be computed incrementally. Cavity expansion theory (Yu and Houlsby, 1991) states that the elastic relationship between radial displacement of a cylindrical cavity in an infinite soil mass and a pressure increase at the cylinder wall is:

$$\Delta s = \frac{\Delta \sigma_n R}{2G} \quad (2)$$

where  $\Delta \sigma_n$  is the incremental normal stress increase (pressure increase),  $G$  is the elastic soil shear modulus and  $R$  is the cylinder radius.

Combining Equations (1) and (2) and rearranging, a relationship between incremental vertical displacement and radial normal stress on the pile-soil interface is derived:

$$\Delta \sigma_n = 2\Delta w \frac{G}{R} \tan \psi \quad (3)$$

\*Corresponding Author

<sup>1</sup>Loadtest Inc., 2631-D NW 41st Street, Gainesville FL, 32606, USA  
Tel:+1 352 378 3717, jon@loadtest.com

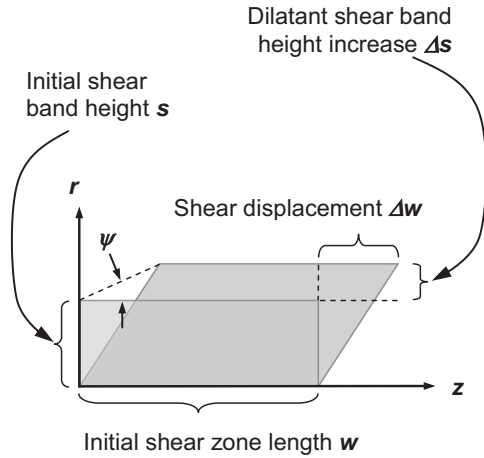


Figure 1. Dilatant Shear Band

Assuming a cohesionless material and a friction angle  $\phi$ , the incremental vertical shear stress increase can be approximated as a function of displacement and pile radius via the Mohr Coulomb relationship:

$$\Delta\tau = \Delta\sigma_n \tan \phi = 2\Delta w \frac{G}{R} \tan \psi \cdot \tan \phi \quad (4)$$

The second phenomenon, related to the first but more applicable to full-scale piles socketed in rock, is the roughness of the pile-soil interface, usually described in relative terms to the radius of the pile. This roughness factor is particularly relevant in rock sockets, where the drilling technique may produce a relatively smooth or rough shaft wall. Seidel and Collingwood (2000) present a shaft roughness coefficient (SRC), given as:

$$SRC = \eta_c \frac{n}{1 + \nu} \frac{\Delta r}{2R} \quad (5)$$

where  $\eta_c$  is an empirical construction method factor,  $n$  is the ratio of rock mass modulus to the unconfined compressive rock strength ( $E_m/q_u$ ),  $\Delta r$  is the mean roughness height and  $\nu$  is the rock Poisson's ratio. Increasing the value of the SRC correlates with increasing interlock between the pile and surrounding rock, which results in a higher ultimate shear capacity.

The third phenomenon, based on the analysis of Randolph and Wroth (1978), models the pile as a cylinder of radius  $R$  embedded in an elastic half-space. The vertical shear at any radial distance  $r$  from the cylinder wall  $\tau_{R+r}$  can be expressed as:

$$\tau_{R+r} = \frac{\tau_R R}{G(R+r)} \quad (6)$$

where  $\tau_R$  is the vertical shear at the cylinder boundary (see Figure 2).

This analysis assumes perfect adhesion between the pile surface and the surrounding soil. The shear stress imposed at the soil interface by the displaced pile is dissipated into the

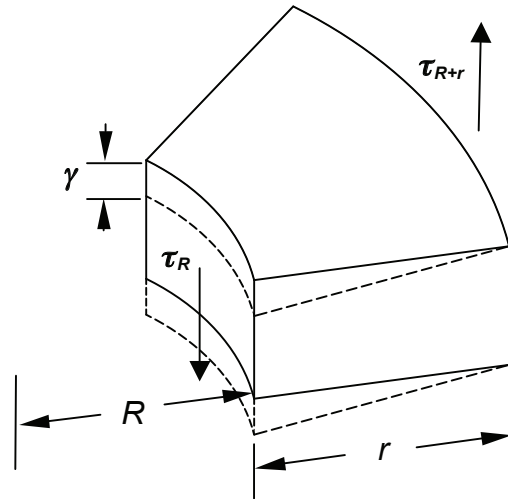


Figure 2. Schematic of Analysis Proposed by Randolph and Wroth.

surrounding soil mass due to radial attenuation. By definition, the vertical shear is also given as:

$$\tau = G\gamma \quad (7)$$

where  $\gamma$  is the shear strain, which can be written as a function of radius:

$$\gamma_r = \frac{\tau_R R}{G(R+r)} \quad (8)$$

The settlement is computed by integrating Eq. (8):

$$w = \int_R^S \gamma_r dr = \frac{\tau_R R}{G} [\ln(R+S) - \ln(R)] = \frac{\tau_R R}{G} \ln\left(\frac{R+r}{R}\right) \quad (9)$$

$$= \frac{\tau_R R}{G} \ln\left(1 + \frac{S}{R}\right)$$

The settlement is dependent on the maximum radius  $S$  to which the definite integral in Eq. (9) is performed. As  $S$  approaches infinity, so does  $w$ . However, if  $S$  is taken as some finite value at which the shear  $\tau_{R+S}$  becomes insignificant or infinitesimal, it can be assumed that no further shearing and therefore no additional settlement takes place.

The value of  $S$  is variously given in the literature by the formulas given by Randolph and Wroth (1978):

$$S = 2.5(1 - \nu)L \quad (10)$$

Fleming et. al. (1992):

$$S = \{.25 + [2.5(1 - \nu) \frac{G_{avg}}{G_L} - .25] \frac{G_L}{G_B}\} L \quad (11)$$

and Scott (1981):

$$S = 50 R \quad (12)$$

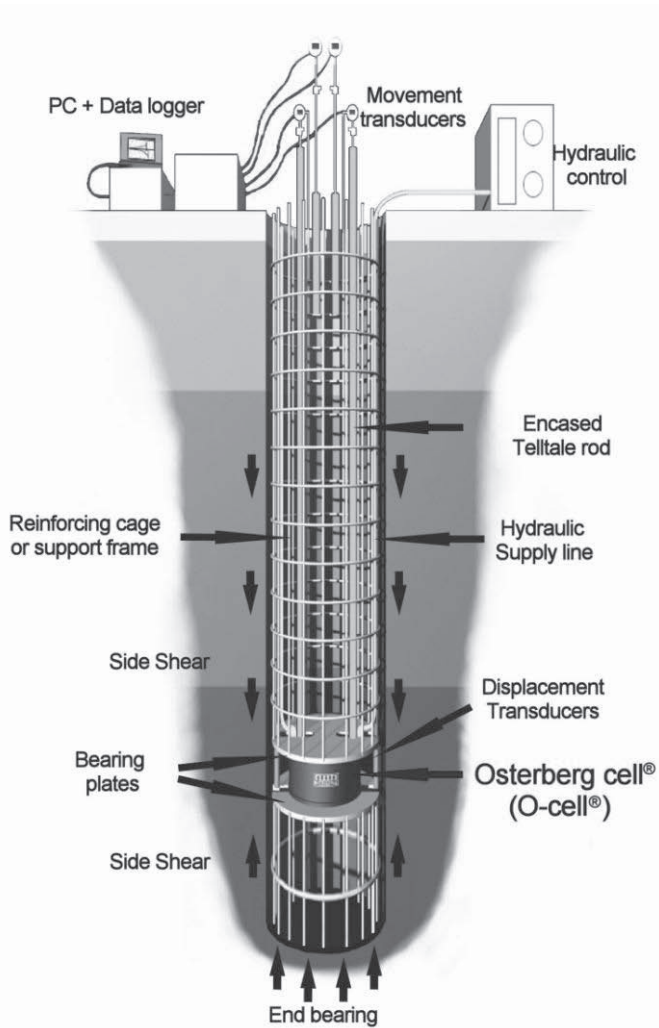


Figure 3. Schematic of O-cell Test Setup.

where  $L$  is the pile length,  $\nu$  is the soil Poisson's ratio, and  $G_{avg}$ ,  $G_L$  and  $G_B$  are the shear moduli of the soil at the mid-point of the pile, tip of pile, and of the material below the pile tip, respectively. Assuming a value for  $\nu$  of 0.2, and  $G_B = G_L$  (uniform material at and below pile tip), then for  $G_{avg} = \frac{1}{2} G_L$  the above Eq. (11) reduces to  $S = L$ . If  $G_{avg} = G_L$ , the result is  $S = 2L$  (the same as for Eq. (10)). Thus, the zone of influence of vertical shearing is influenced by, and approximately on the same order of magnitude, as the length of the pile. Eq. (12) simplifies Eq. (9) to a straightforward linear relationship between settlement  $w$  and pile radius  $R$ . Eq. (9) can be re-written as:

$$\tau_R = \frac{w}{\ln\left(1 + \frac{S}{R}\right)} \frac{G}{R} \quad (13)$$

Cooke and Price (1973) reported the vertical displacements within a soil column around an axially-loaded pile.

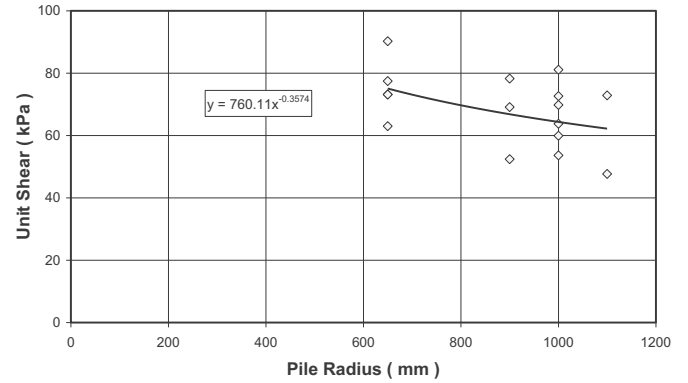


Figure 4. Unit Shear vs. Pile Radius at 4 mm displacement - Changi Water Treatment Plant - Singapore.

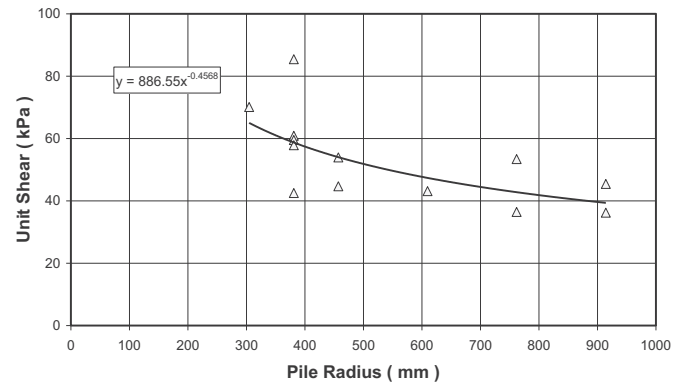


Figure 5. Unit Shear vs. Pile Radius at 6.25 mm displacement - Downtown/Brickell Area - Miami, Florida.

These measurements, which indicate significant vertical displacements of the soil surface out to greater than 12 pile radii, support the deformation analysis presented above.

Examining Equations (4), (5) and (13), it is interesting to note that for all three scaling phenomena described in the literature, the radius of the pile is in the denominator of the computation of unit shear. Thus, the scaling factor is explicit in all three models. Equations (4) and (13) (describing phenomena 1 and 3) also explicitly relate this calculation to a given displacement.

Note that the equations presented from the literature above have certain limitations. The dilatant phenomenon generally relates to small-scale tests, where individual soil grain size becomes a factor. The derivation by Randolph & Wroth is based on linear elastic theory and is a simplifying model. For example, taking the analysis to its extreme implies that the face of an infinite embedded wall (modeled as a pile of infinite radius) has no shear strength.

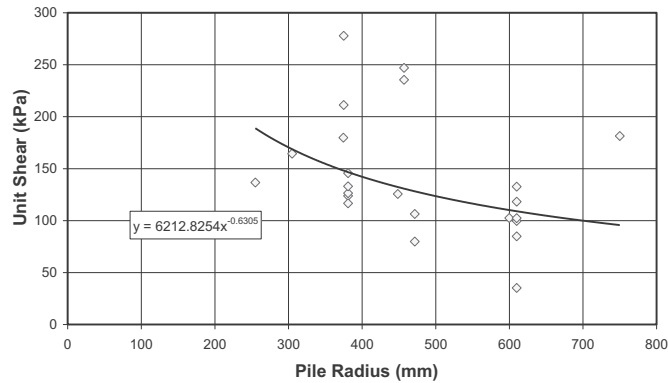


Figure 6. Unit Shear vs. Pile Radius at 5 mm displacement - McMurray Formation Oilsand.

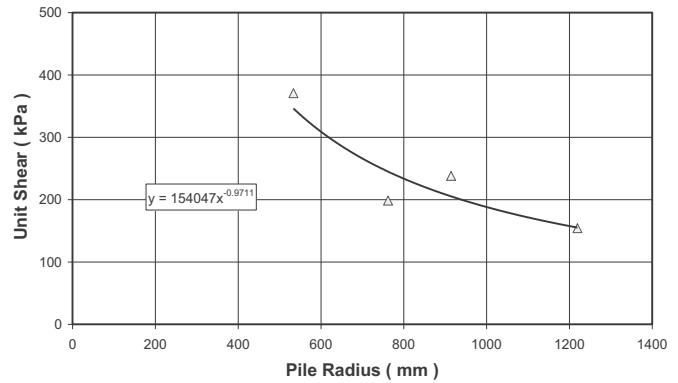


Figure 8. Unit Shear vs. Pile Radius at 6.25 mm displacement - New Jersey Sandstone.

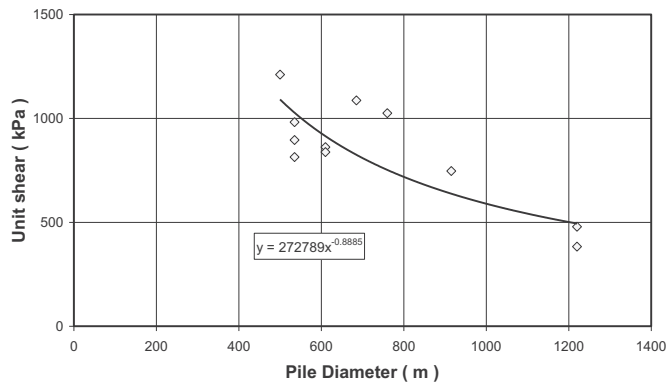


Figure 7. Unit Shear vs. Pile Radius at 5 mm displacement - Shale (from Hayes (2008), p. 645, Table 3, Figure 7 (“Medium Shale”).

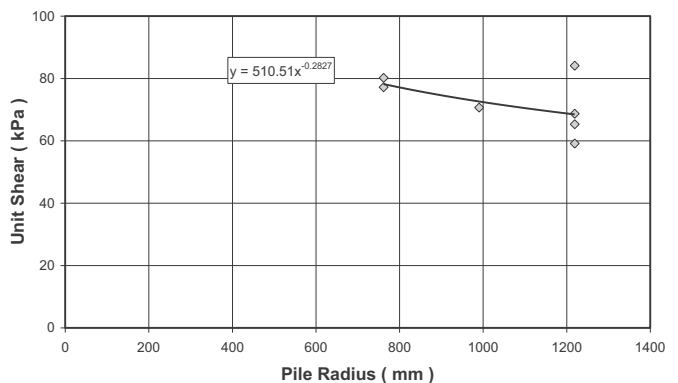


Figure 9. Unit Shear vs. Pile Radius at 6.25 mm displacement - Cooper Marl Formation.

### 3. FULL-SCALE TEST DATA:

The O-cell is a hydraulically driven, high capacity, sacrificial loading device installed within the bored pile (see Figure 3). As hydraulic pressure is applied to the O-cell, it exerts load in two directions; upward against upper side shear and downward against base resistance and lower side shear (if applicable). The O-cell derives all reaction from the surrounding soil and/or rock. End bearing provides reaction for the skin friction portion of the O-cell load test, and skin friction provides reaction for the end bearing portion of the test. Load testing with the O-cell continues until one of three things occurs: ultimate skin friction capacity is reached, ultimate end bearing capacity is reached, or the maximum O-cell capacity is reached.

Data plots (Figures 4 – 9) have been collected from various areas where data are available for multiple tests on piles of various radii in a geographically and/or geologically similar area (LOADTEST 1995-2010). Due to the fact that the data are collected from field tests conducted on piles often

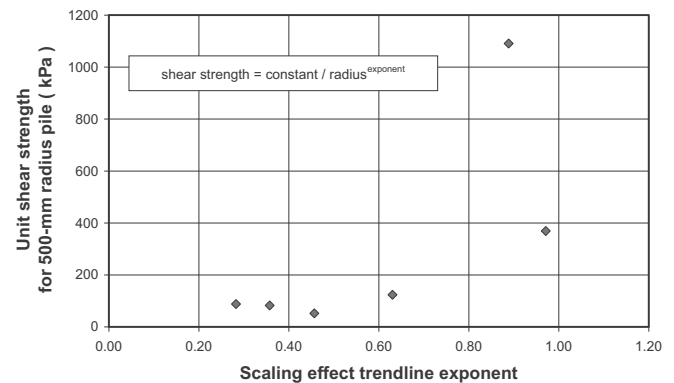


Figure 10. Unit Shear Strength vs. Trendline Exponent (at ~5 mm displacement).

constructed at different sites by various contractors employing diverse construction techniques, there is significant scatter in the data. However, regardless of the soil type or construction techniques, the trend of decreasing unit shear as radius increases (at a fixed pile displacement) holds. Note

that, based on the form of Equations (4), (5) and (13) above, the trendlines fit to the data are assumed to be inverse power functions of the form  $U = a/R^b$ . The constants  $a$  and  $b$  are adjusted using the method of least squares to achieve the best fit for each data set.

Figure 10 illustrates a meta analysis comparing the inverse relationship of radius to unit shear, at a displacement of approximately 4 to 6 mm. The strength of the inverse relationship appears to be correlated to the relative strength of the soils.

#### 4. CONCLUSIONS

Note that all data presented herein was collected from bored pile (drilled shaft) and auger-cast pile tests, and the conclusions presented herein may not be appropriate for displacement piles. The scaling effect appears to be a quantifiable phenomenon in bored piles. Since results from smaller radius pile load tests are often used for the design of larger-radius production piles, it may be advisable to scale the unit shear capacity by the ratio of the radii to conservatively account for the scaling effect at a given displacement, especially when working in stiffer soil materials. However, considering the scatter in the data presented herein, testing of full scale piles to eliminate uncertainty due to scaling effect may be the best solution.

Drilled shaft capacity is often defined at a settlement given as a percentage of the shaft diameter, rather than at a fixed displacement. This may be an implicit acknowledgement by the industry of the scaling effect. If the only concern is ultimate capacity, then the scaling effect may not be very important. However, modern design methods often incorporate software to compute load distribution and deformation for an integrated structural model which may include multiple pile and pile cap elements. Such analyses model the soil-structure interaction via nonlinear springs. In order to correctly analyze the load transfer mechanism of the structure, the springs must have the correct stiffness both at small and large displacements. It is thus important to keep the scaling effect in mind when using test data to calibrate or validate computer model inputs.

#### REFERENCES

- Balachowski, L. (2006) "Scale Effect in Shaft Friction from the Direct Shear Interface Tests," *Archives of Civil and Mechanical Engineering*, VI (3), 13-28.
- Bolton, M. D. (1986) "The Strength and Dilatancy of Sands," *Géotechnique*, 36(1), 65-78.
- Boulon, M and Foray, P. (1986) "Physical and Numerical Simulation of Lateral Shaft Friction along Offshore Piles in Sand," *Proceedings of the 3rd International Conference on Numerical Methods in Offshore Piling*, Nantes, 127-147.
- Cooke, R. W. and Price, G. (1973) "Strains and Displacements around Friction Piles," *Proceedings of the 8th International Conference on Soil Mechanics and Foundation Engineering*, Moscow, Vol. 2, 53-60.
- Fleming, W. G. K., Weltman, A. J., Randolph, M. F. and Elson, W. K. (1992) *Piling Engineering*, Surrey University Press, Surrey UK.
- Garnier, J. and König, D. (1998) "Scale Effects in Piles and Nails Loading Tests in Sand," *Proceedings of the International Conference Centrifuge 98*, Tokyo, Vol. 1, 205-210.
- Hayes, J. A. (2008) "The Quest for Quality in Deep Foundations", From Research to Practice in Geotechnical Engineering, *ASCE GeoInstitute Geotechnical Special Publication No. 180*, 636-652.
- Hettler, A. (1982) "Approximation Formulae for Piles Under Tension," *IUTAM Conference on Deformation and Failure of Granular Materials*, Delft, 603-608.
- LOADTEST Inc., (1995-2010) *Osterberg Cell Test Database*, Gainesville, FL.
- Marandi, S.M. and Karimzadeh, M. A. (2009) "Analysis of the Effect of Pile Skin Resistance Versus Pile Diameter Based on Experimental Research," *American Journal of Applied Sciences*, 6(1), 114-123.
- Randolph, M. F. and Wroth, C. P. (1978) "Analysis of Deformation of Vertically Loaded Piles," *Journal of the Geotechnical Engineering Division*, ASCE, 104(12), 1465-1488.
- Scott, R. F. (1981) *Foundation Analysis*, Prentice-Hall, New Jersey.
- Seidel, J.P. and Collingwood, B. (2000) "A New Socket Roughness Factor for Prediction of Rock Socket Shaft Resistance," *Canadian Geotechnical Journal*, 38, 138-153.
- Vermeer, P. A. and Luger, H. J. (1982) "Deformation and Failure of Granular Materials," *Proceedings of the IUTAM Symposium on Deformation and Failure of Granular Materials*, Delft, 603-608.
- Wernick, E. (1977) "Stresses and Strains on the Surface of Anchors," *Revue Française de Géotechnique*, Special Edition on Anchors, 113-119.
- Yu, H. S. and Houlsby, G. T. (1991) "Finite Cavity Expansion in Dilatant Soils: Loading Analysis," *Géotechnique*, 41(2), 173-183.